Mitochondrion 89 (2026) 102152

Contents lists available at ScienceDirect

Mitochondrion

journal homepage: www.elsevier.com/locate/mito

Original Research Article

Mitochondrial DNA analysis in a cohort of stillbirths with brainstem and cardiac conduction system abnormalities

Mauro Lecca [a], Nicolò Mele [a], Patrizia Leonardi [b], Giulia Ottaviani [b], Edoardo Errichiello [a,c,*]

[a] Unit of Medical Genetics, Department of Molecular Medicine, University of Pavia, Pavia, Italy
[b] Anatomic Pathology, Lino Rossi Research Center, Department of Biomedical, Surgical and Dental Sciences, University of Milan, Milan, Italy
[c] Neurogenetics Research Center, IRCCS Mondino Foundation, Pavia, Italy

ARTICLE INFO

Keywords:
Stillbirth (SB)
Brainstem
cardiac conduction system (CCS)
mitochondrial DNA (mtDNA)
mitochondrial DNA copy number (mtDNA-CN)
displacement loop (D-loop)
Methylation

ABSTRACT

Stillbirth (SB) accounts for over 60% of perinatal deaths in high-income countries, with a significant portion of cases remaining unexplained following thorough anatomopathological investigation. Mitochondrial DNA (mtDNA) alterations were analyzed in 42 SB cases with brainstem and cardiac conduction system (CCS) anomalies and in 32 control fetuses without these anomalies. DNA extracted from brainstem tissues was analyzed in both groups. In addition, unaffected tissues from the SB cases were examined for intra-individual comparison. The analysis included mtDNA sequencing, haplogroup determination, copy number (CN) quantification, and evaluation of displacement loop (D-loop) instability and methylation.

Across the entire SB cohort, a total of 158 variants were identified, with a significant enrichment of variants observed in cases without CCS anomalies ($p = 0.024$). Affected brainstem tissues exhibited significantly higher mtDNA-CN compared with both control brainstem tissues ($p < 0.0001$) and unaffected tissues ($p = 0.005$), with levels higher in mild lesions than in severe lesions ($p = 0.02$). D-loop instability was identified in 37% of cases, and D-loop methylation levels were consistently higher in affected brainstem tissues compared with both control brainstem tissues ($p < 0.0001$) and unaffected tissues ($p = 0.0001$). These findings support mitochondrial dysfunction as a key contributor to fetal demise and mtDNA-CN as a potential biomarker for SB.

1. Introduction

Stillbirth (SB) accounts for over 60% of perinatal deaths (Stanley et al, 2020) and occurs more frequently in developed countries than in developing ones (Dolanc Merc et al., 2023); cases occurring after 28 weeks of gestation (wog) are classified as late SB. Fetal autopsy and genetic investigations, primarily conventional karyotype and/or chromosomal microarray analysis (CMA), are routinely performed to investigate the causes of SB; however, a substantial proportion of fetuses (25–50%) show no detectable abnormalities (Giorlandino et al., 2012), a condition known as sudden intrauterine unexplained death syndrome (SIUDS). Previous in-depth post-mortem investigations have revealed brainstem microlesions and defects in the cardiac conduction system (CCS) in SIUDS cohorts (Lavezzi et al., 2016, Ottaviani, 2016). Furthermore, it has been suggested that these anomalies may trigger adaptive metabolic processes, including increased mitochondrial biogenesis (Lattuada et al., 2018). Multiple lines of evidence suggest a link between mitochondrial dysfunction and these anatomopathological anomalies. First, the brainstem and heart are organs with high energy demand and are commonly affected in subjects with mitochondrial disorders. Second, mitochondrial function is critical during pregnancy, and SB has been reported as a potential complication in women with mitochondrial disease/dysfunction (Karaa et al., 2019; Feeney et al., 2019; Hui et al., 2025). Finally, variants affecting mitochondrial genes that encode respiratory chain enzymes (Vanniarajan et al., 2011), alterations in the non-coding regulatory displacement loop (D-loop) region (Seyedhassani et al., 2010), and changes in mitochondrial DNA (mtDNA) copy number (mtDNA-CN) (Danusso et al., 2022, Diez-Juan et al., 2015) have been reported in cases of pregnancy loss (Ye et al., 2020) and SIUDS (Lattuada et al., 2018). Based on this evidence, mtDNA has been proposed as a promising biomarker for SIUDS (Lattuada et al., 2018).

* Corresponding author at: Unit of General Biology and Medical Genetics, Department of Molecular Medicine, University of Pavia,Via C. Forlanini, 14 – 27100, Pavia, Italy.
E-mail address: edoardo.errichiello@unipv.it (E. Errichiello).

https://doi.org/10.1016/j.mito.2026.102152
Received 28 October 2025; Received in revised form 16 March 2026; Accepted 31 March 2026
Available online 2 April 2026

In this study, we investigated mtDNA alterations from multiple perspectives, including mtDNA variants, mtDNA-CN, D-loop instability, and D-loop methylation, in a homogeneous, monocentric Italian cohort of SB exhibiting brainstem and CCS anomalies.

2. Samples and methods

2.1. Samples

This study cohort included 42 unrelated SB cases with brainstem and CCS abnormalities (mean gestational age: 37.1 ± 4 weeks; range: 28–41.5 weeks), including 24 males and 18 females. The control group consisted of 32 unrelated fetuses without these abnormalities (mean gestational age: 27.8 ± 7 weeks; range: 18–41.4 weeks), including 16 females and 16 males. All samples were collected at the "Lino Rossi Research Center" of the University of Milan between 2008 and 2022. No macroscopic morphological abnormalities were detected in any of the selected samples. Examination of the placental disk, umbilical cord, membranes and review of maternal clinical history yielded no significant findings in SB cases. In-depth examination of the autonomic nervous system in SB cases revealed alterations of the brainstem centers responsible for regulating vital cardiac and respiratory functions, including fetal breathing movements (FBMs) (Fig. S1 and Fig. S2). Specifically, hypoplasia was observed in the arcuate nucleus, Kölliker-Fuse nucleus, raphe nuclei, and the pre-Bötzinger complex. Approximately three-quarters of cases (32/42) displayed CCS defects, especially Mahaim fibers (21/32, 66%). Many of the brainstem abnormalities were classified as severely affecting crucial structures within the so-called "respiratory network" (RN) (Lavezzi et al., 2016). Conversely, other neuropathological findings were considered mild, since similar anomalies may be detected in adults who die from known causes, indicating that they are compatible with neonatal life and unlikely to result in SB (Lavezzi et al., 2004; Matturri et al., 2008; Paradiso et al., 2018). The examination of serial sections of the brainstem in the control cases did not reveal any lesions.

The concomitant presence of brainstem lesions and CCS anomalies was observed in 26 SBs with severe lesions and in 6 SBs with mild lesions. Subgroup stratification was performed according to sex, severity of brainstem anomalies, and the presence or absence of concomitant CCS defects.

Brainstem specimens were collected from both SB cases and controls. In addition, available unaffected tissues (e.g., thymus) from SB cases were examined to enable intra-individual comparison.

Additional information on cases and controls is summarized in Tables 1 and 2, respectively.

2.2. DNA extraction and mtDNA sequencing

DNA was extracted from formalin-fixed paraffin-embedded (FFPE) brainstem and unaffected tissues (20 μm sections) using the QIAamp DNA FFPE Advanced UNG Kit (Qiagen, Hilden, Germany), according to manufacturer's instructions with minor modifications. All DNA samples underwent rigorous quality control (QC), including assessment of DNA degradation, concentration and purity (NanoDrop, Qubit), and *SRY*-based sex determination to confirm anatomical sex. Mitochondrial DNA (mtDNA) sequencing was successfully performed in 34 out of 42 SB cases (8 samples were excluded due to QC failure after library preparation) using the Twist Mitochondrial Panel (Twist Bioscience, San Francisco, CA, USA) on a NovaSeq 6000 platform (Illumina, San Diego, CA, USA).

2.3. Detection of mtDNA variants

Bioinformatic analysis focused on variants within the 37 genes of the mitochondrial genome with a minor allele frequency (MAF) < 5% according to gnomAD v.4.1.0 and dedicated mitochondrial databases such as MITOMAP (https://www.mitomap.org) and mtDB (https://www.genepat.uu.se/mtDB). *In-silico* pathogenicity predictions were performed using HmtVar (Preste et al., 2019), APOGEE2 (Bianco et al., 2023), and MitoTIP (Sonney et al., 2017). All candidate variants were classified according to the ACMG/AMP guidelines for mtDNA variant interpretation (McCormick et al., 2020). Mutational burden for each sample was calculated as the number of variants per total mtDNA length (in base pairs, bp). Mitochondrial haplogroups were assigned using Haplogrep 3 (https://haplogrep.i-med.ac.at/) (Schönherr et al., 2023) in SB cases and in 107 samples from the Tuscan Italians (TSI) population of the 1000 Genomes Project (phase 3 release), used as a reference for the Italian population.

2.4. Quantification of mtDNA copy number (mtDNA-CN)

mtDNA content was evaluated by using the Absolute Human Mitochondrial DNA Copy Number Quantification qPCR Assay Kit (Science Cell, Carlsbad, CA, USA), on a CFX 96 real-time PCR detection system (Bio-Rad, Milan, Italy), following the manufacturer's instructions. For each sample, the $2^{-\Delta\Delta Cq}$ method was applied, and absolute mtDNA-CN was calculated accordingly.

2.5. D-loop instability and methylation analysis

To assess D-loop instability, we used primers (5′-ACCTACGTTCAATATTACAGGCG-3′ and 5′-CTGTGGGGGGTGTCTTTGGGG-3′; Xu et al., 2012) to amplify the hypervariable poly-C stretch between positions m.303–m.315 (C7-T-C5) within the D310 region, a known hypervariable hotspot characterized by frequent sequence insertions and deletions. Comparison of D-loop poly(C) instability between affected brainstem tissues and unaffected tissues in SB cases was performed as previously reported (Errichiello et al., 2015).

D-loop methylation levels were assessed using a methylation-sensitive high-resolution melting (MS-HRM) assay. Briefly, 500 ng of DNA was bisulfite-converted using the EpiTect Bisulfite Kit (Qiagen), following the manufacturer's protocol. MS-HRM amplification was carried out as previously reported (Stoccoro et al., 2022). A standard curve was generated using reference DNA samples with known methylation % (0, 12.5, 25, 37.5, 50, 62.5, 75, 87.5, and 100%), prepared by mixing fully methylated and unmethylated control DNA (EpiTect PCR Control DNA Set, Qiagen). The % of methylation for each sample was calculated by interpolating the fluorescence derivative value (−d(RFU)/dT) onto the standard curve, as described by Migheli et al. (2013).

2.6. Statistical analysis

Differences in mean mtDNA-CN, D-loop methylation, and mutational burden were assessed using unpaired t-tests for comparisons between SB cases and controls and across cohort subgroups (e.g., sex, presence/absence of CCS defects, and severity of brainstem anomalies), whereas two-tailed paired t-tests were used for intra-individual comparisons (affected brainstem tissues vs. unaffected tissues). All statistical analyses were performed using GraphPad Prism version 10.4.2 (GraphPad Software, San Diego, CA, USA), with $p < 0.05$ considered statistically significant.

3. Results

3.1. mtDNA variants and haplogroups

Analysis of mtDNA mutational burden identified a total of 158 variants across all examined samples. The number of variants per sample ranged from 1 (e.g., SB6 and SB26, corresponding to a mutational burden of 0.006%) to 27 variants (SB29, 0.16%) with a mean of approximately 4.64 variants per sample (0.027%) (Table 1). Notably, mtDNA variants were more frequent in SBs without CCS anomalies (52

Table 1
Demographic, clinical, and molecular findings of the SB cohort. M = Male; F = Female; wog = weeks of gestation.

Case	Affected tissue	Unaffected tissue	Anatomical sex	Age (wog)	Brainstem anomalies (severe lesions in bold)	CCS anomalies	mtDNA mutational burden	Haplogroup (concordance %)	mtDNA-CN		D-loop methylation (%)		D-loop D310 instability
									Affected tissue	Unaffected tissue	Affected tissue	Unaffected tissue	
SB1	Obex	Thymus	M	39 + 2	**Severe hypoplasia of the Kölliker-Fuse nucleus and the pre-Bötzinger complex**	Alterations in the morphogenesis of high-potential arrhythmogenic junctional tissue	6/16569 (0.036%)	M35b2*1a (101%)	2998	1038	9.7	5.1	No
SB2	Obex	Thymus	M	28 + 0	**Hypoplasia of the facial/ parafacial complex in the caudal pons**	Presence of Mahaim fibers	10/16569 (0.06%)	U2e2a1a (98%)	4904	251	10.3	7.8	No
SB3	Obex	Thymus	M	41 + 5	**Hypoplasia of the arcuate nucleus and caudal raphe group nuclei**	/	7/16569 (0.042%)	H1e1a5 (85%)	7803	690	8.1	7.2	Yes
SB4	Pons	Thymus	F	41 + 0	**Severe hypoplasia of the Kölliker-Fuse nucleus**	Intramural bifurcation, right bundle branch hypoplasia	6/16569 (0.036%)	H4a1 (92%)	7803	102	9.1	4.7	No
SB5	Obex	Thyroid	M	40 + 0	**Hypoplasia of the Kölliker-Fuse nucleus; hypoplasia of all raphe nuclei; hypoplasia of the arcuate nucleus**	Noncompact ventricular cardiomyopathy, hypoplasia of the central fibrous body	3/16569 (0.018%)	H12a (89%)	4240	1687	11.7	6.8	Yes
SB6	Obex	Lungs	M	40 + 6	**Hypoplasia of the Kölliker-Fuse nucleus in the rostral pons and caudal mesencephalon**	Intramural bifurcation, hypoplasia of the right bundle branch	1/16569 (0.006%)	J1c2o (100%)	4640	685	7.1	4.5	No
SB7	Obex	Thymus	M	38 + 6	**Severe hypoplasia of the lateral intermediate nucleus of the spinal cord**	Alterations in junctional tissue morphogenesis	3/16569 (0.018%)	K1a (90%)	6653	169	7.9	7.3	No
SB8	Obex	Thyroid	M	36 + 5	**Severe hypoplasia of the Kölliker-Fuse nucleus**	Cardiac conduction system abnormalities (unspecified)	0/16569 (0%)	H (92%)	3147	1618	7.9	9.5	No
SB9	Obex	Thyroid	F	38 + 0	**Hypoplasia of the Kölliker-Fuse and hypoplasia of the pre-Bötzinger nucleus**	Alterations in junctional tissue morphogenesis, presence of Mahaim fibers	2/16569 (0.012%)	U5b1b1 (92%)	5752	1746	8.2	7.5	Yes
SB10	Obex	Thymus	F	39 + 6	**Hypoplasia of the raphe nuclei in the medulla oblongata**	Alterations in junctional tissue morphogenesis, presence of Mahaim fibers	2/16569 (0.012%)	H5 (86%)	9877	549	6.3	7.9	No
SB11	Obex	Thymus	M	38 + 4	**Hypoplasia of the pre-Bötzinger nucleus and right unilateral hypoplasia of the arcuate nucleus**	Ectopic and dual conduction beats responsible for lethal cardiac arrhythmias	8/16569 (0.048%)	U4a (96%)	11,910	249	7.9	8.1	Yes
SB12	Obex	Thymus	M	40 + 1	**Hypoplasia of the parafacial/ retroptrapezoid/superior olivary complex and agenesis of the arcuate nucleus**	Alterations in junctional tissue morphogenesis, presence of Mahaim fibers	2/16569 (0.012%)	H1b1 (88%)	4211	160	7.5	4.6	No

(*continued on next page*)

Table 1 (*continued*)

Case	Affected tissue	Unaffected tissue	Anatomical sex	Age (wog)	Brainstem anomalies (severe lesions in bold)	CCS anomalies	mtDNA mutational burden	Haplogroup (concordance %)	mtDNA-CN		D-loop methylation (%)		D-loop D310 instability
									Affected tissue	Unaffected tissue	Affected tissue	Unaffected tissue	
SB13	Caudal medulla oblongata	Thymus	F	38 + 2	**Hypoplasia of the pre-Bötzinger nucleus and in the cervical portion of the spinal cord hypoplasia of the lateral intermediate nucleus**	Atrioventricular junctional cardiac conduction system abnormalities	2/16569 (0.012%)	K1a2a (96%)	7537	244	10.0	5.1	Yes
SB14	Pons	Thymus	F	32 + 0	**Hypoplasia of the facial/parafacial complex and of the middle nucleus of the superior olivary complex**	Atrioventricular nodal hyperplasia with compression of the central fibrous body, presence of Mahaim fibers	2/16569 (0.012%)	HV (72%)	8248	205	6.8	6.4	Yes
SB15	Obex	Thymus	F	40 + 0	**Developmental alterations of nervous structures that regulate chemoreception and serotonin synthesis**	Mild abnormalities of the cardiac conduction system	3/16569 (0.018%)	HV + 73 (78%)	7180	832	8.9	7.2	No
SB16	Obex	Thymus	M	40 + 4	**Hypoplasia of the facial/parafacial complex, moderate hyperplasia of the locus coeruleus**	/	n.a. (failed)	/	6984	59	11.7	7.3	No
SB17	Obex	Thymus	F	36 + 3	**Hypoplasia of the Kölliker-Fuse nucleus**	Dualism of the sinoatrial node, presence of Mahaim fibers	2/16569 (0.012%)	HV7 (96%)	14,065	189	7.2	7.3	No
SB18	Obex	Thymus	M	34 + 1	Mild hypoplasia of the arcuate nucleus and raphe nuclei	Congenital cardiac anomalies potentially arrhythmogenic, presence of Mahaim fibers, fetal thrombotic vasculopathy	4/16569 (0.024%)	U5b3h(90%)	8305	495	5.4	4.7	No
SB19	Obex	Thymus	F	38 + 4	**Hypoplasia of the Kölliker-Fuse nucleus, hypoplasia of the obscurus and pallidus raphe nuclei, agenesis of the arcuate nucleus**	Mahaim fibers, fetal thrombotic vasculopathy	7/16569 (0.042%)	H1u (81%)	10,513	916	16.7	8.8	No
SB20	Obex	Thymus	F	39 + 3	**Developmental alterations of all raphe nuclei**	Intramural cardiac bifurcation, presence of Mahaim fibers, fetal thrombotic vasculopathy	3/16569 (0.018%)	H1z1 (93%)	8421	373	13.8	11.7	No
SB21	Obex	Thymus	M	40 + 4	**Hypoplasia of the pre-Bötzinger nucleus**	Potentially arrhythmogenic alterations, presence of Mahaim fibers	3/16569 (0.018%)	H49a (87%)	21,918	471	9.5	4.7	Yes
SB22	Obex	Thymus	F	38 + 6	**Hypoplasia of the Kölliker-Fuse nucleus and the facial/parafacial complex**	Congenital arrhythmogenic alterations of the cardiac conduction system, presence of Mahaim fibers	2/16569 (0.012%)	H6a1b4 (95%)	8718	488	6.8	6.1	Yes

(*continued on next page*)

Table 1 (*continued*)

Case	Affected tissue	Unaffected tissue	Anatomical sex	Age (wog)	Brainstem anomalies (severe lesions in bold)	CCS anomalies	mtDNA mutational burden	Haplogroup (concordance %)	mtDNA-CN		D-loop methylation (%)		D-loop D310 instability
									Affected tissue	Unaffected tissue	Affected tissue	Unaffected tissue	
SB23	Obex	Thymus	F	35 + 0	**Agenesis of the pontine nucleus of Kölliker-Fuse, severe hypoplasia of all raphe nuclei**	Congenital arrhythmogenic alterations of the junctional system, presence of Mahaim fibers	2/16569 (0.012%)	H3e (100%)	11,910	272	11.5	8.6	No
SB24	Obex	Thymus	M	40 + 3	**Hypoplasia of the facial/ parafacial complex**	Congenital arrhythmogenic alterations of the junctional system, presence of Mahaim fibers	2/16569 (0.012%)	H39a1 (85%)	26,985	1351	12.3	9.1	Yes
SB25	Obex	Lungs	M	36 + 2	**Hypoplasia of the facial/ parafacial complex and medullary raphe nuclei; agenesis of the lateral intermediate nucleus of the spinal cord.**	/	3/16569 (0.018%)	H5a1 (87%)	8779	1418	8.8	6.2	No
SB26	Obex	Thymus	M	39 + 5	**Hypoplasia of the facial/ parafacial complex and the retrotrapezoid nucleus, hypoplasia of the caudal raphe nuclei, hypoplasia of the lateral intermediate nucleus**	/	1/16569 (0.006%)	K1a2 (93%)	11,910	57	10.1	11.5	Yes
SB27	Obex	Thymus	M	39 + 0	**Hypoplasia of the arcuate nucleus, hypoplasia of the inferior olivary nucleus and of all raphe nuclei**	/	n.a. (failed)	/	11,906	298	11.6	8.5	No
SB28	Obex	Cerebellum	M	33 + 0	**Hypoplasia of the arcuate nucleus, of all raphe nuclei and of the pre-Bötzinger complex**	/	11/16569 (0.066%)	W6 (93%)	12,244	4067	8.8	8.9	No
SB29	Obex	Thymus	M	39 + 0	**Hypoplasia of the arcuate nucleus, pre-Bötzinger nucleus, and facial/ parafacial complex**	/	27/16569 (0.16%)	L1b1a18 (94%)	1218	576	7.5	7.2	No
SB30	Obex	Thymus	F	36 + 4	Mild hypoplasia of the arcuate nucleus	Non-compact cardiomyopathy of the left ventricle, presence of Mahaim fibers	n.a. (failed)	/	15,934	5042	6.9	9.4	No
SB31	Obex	Thymus	M	40 + 4	**Hypoplasia of the facial/ parafacial complex, mild hypoplasia of the arcuate nucleus**	Presence of Mahaim fibers	8/16569 (0.048%)	J2b1g (98%)	10,734	622	9.7	9.8	No
SB32	Obex	Hearth ventricle	M	37 + 0	**Hypoplasia of the Kölliker-Fuse nucleus and of the pre-Bötzinger nucleus**	/	3/16569 (0.018%)	V (93%)	8480	81,802	9.9	7.0	Yes
SB33	Obex	Thymus	M	28 + 0	**Delayed maturation of the ependimal lining of**	Presence of areas of atrioventricular node dispersion, areas of	3/16569 (0.018%)	T1a + 152 (96%)	5873	181	9.7	6.8	Yes

(*continued on next page*)

Table 1 (*continued*)

Case	Affected tissue	Unaffected tissue	Anatomical sex	Age (wog)	Brainstem anomalies (severe lesions in bold)	CCS anomalies	mtDNA mutational burden	Haplogroup (concordance %)	mtDNA-CN		D-loop methylation (%)		D-loop D310 instability
									Affected tissue	Unaffected tissue	Affected tissue	Unaffected tissue	
					the fourth ventricle and cerebral cortex	junctional tissue in the central fibrous body							
SB34	Obex	Thymus	F	39 + 1	**Hypoplasia of the pontine facial-parafacial/ retrotrapezoid/superior olivary complex hypoplasia of the raphe nuclei in the medulla oblongata**	Presence of Mahaim fibers	n.a. (failed)	/	8718	372	12.1	7.2	Yes
SB35	Obex	Thymus	M	30 + 5	**Hypoplasia of the Kölliker-Fuse**	Islands of glumonic tissue in the central fibrous body	3/16569 (0.018%)	U5a2b3a1 (94%)	7803	302	7.7	8.6	No
SB36	Obex	Thymus	F	38 + 0	**Hypoplasia of the Kölliker-Fuse nucleus and of the raphe nuclei**	Presence of Mahaim fibers	n.a. (failed)	/	4904	221	13.6	10.8	Yes
SB37	Obex	Hearth ventricle	M	33 + 0	**Hypoplasia of the facial/ parafacial complex and of the middle nucleus of the superior olivary complex**	Congenital arrhythmogenic alterations of the cardiac conduction system, presence of Mahaim fibers	n.a. (failed)	/	6122	11,112	6.4	8.7	Yes
SB38	Obex	Thymus	M	39 + 0	Mild underdevelopment of the superior olivary nucleus in the caudal pons	Fetal thrombotic vasculopathy, presence of Mahaim fibers	11/16569 (0.066%)	L3f1b + 16292 + 150 (93%)	9475	564	8.6	5.4	No
SB39	Obex	Thymus	F	34 + 5	Mild underdevelopment of the superior olivary nucleus in the caudal pons	Presence of Mahaim fibers	2/16569 (0.012%)	H14b (82%)	36,354	622	12.1	6.1	No
SB40	Obex	Thymus	F	37 + 3	Mild underdevelopment of the superior olivary nucleus in the caudal pons	Congenital arrhythmogenic alterations of the junctional system, presence of Mahaim fibers	4/16569 (0.024%)	T2b3a1 (91%)	13,123	122	13.3	11.9	No
SB41	/	Thymus	F	28 + 0	Mild hypoplasia of the arcuate nucleus	/	n.a. (failed)	/	Not performed	244	Not performed	7.5	/
SB42	Obex	Cerebellum	F	37 + 4	Mild hypoplasia of the arcuate nucleus	/	n.a. (failed)	/	9215	553	11.5	8.3	No

Table 2
Demographic, anatomical, and molecular findings of controls. M = Male; F = Female; wog = weeks of gestation.

Control	Tissue	Anatomical sex	Age (wog)	mtDNA-CN	D-loop methylation %
CTRL 1	Obex	F	26 + 0	1269.33	5.49
CTRL 2	Obex	F	19 + 0	1341.7	4.00
CTRL 3	Obex	F	33 + 0	1573.59	7.04
CTRL 4	Obex	M	35 + 0	1897.45	4.49
CTRL 5	Obex	M	34 + 0	2134.74	5.32
CTRL 6	Obex	M	38 + 0	792.27	8.00
CTRL 7	Brainstem *in toto*	M	20 + 0	1617.83	7.94
CTRL 8	Brainstem *in toto*	F	20 + 0	885.19	6.90
CTRL 9	Brainstem *in toto*	F	38 + 0	770.6	6.68
CTRL 10	Brainstem *in toto*	F	27 + 0	5256.35	8.93
CTRL 11	Brainstem *in toto*	F	19 + 0	1369.89	12.53
CTRL 12	Brainstem *in toto*	M	35 + 0	2240.87	10.19
CTRL 13	Brainstem *in toto*	M	35 + 4	1732.2	7.87
CTRL 14	Brainstem *in toto*	M	35 + 0	1640.42	5.04
CTRL 15	Brainstem *in toto*	M	30 + 0	2385.12	8.08
CTRL 16	Brainstem *in toto*	F	37 + 0	1759.09	7.52
CTRL 17	Pons	M	20 + 4	948.72	6.79
CTRL 18	Pons	M	34 + 0	2716.85	7.80
CTRL 19	Pons	M	22 + 0	630.28	8.42
CTRL 20	Pons	F	20 + 0	2503.70	10.25
Control	**Tissue**	**Anatomical sex**	**Age (wog)**	**mtDNA-CN**	**D-loop methylation %**
CTRL 21	Pons	F	18 + 0	638.28	10.33
CTRL 22	Pons	M	21 + 0	1766.15	8.03
CTRL 23	Brainstem *in toto*	M	23 + 0	1089.80	7.59
CTRL 24	Pons	F	23 + 3	1783.01	4.40
CTRL 25	Pons	M	20 + 0	1746.01	6.98
CTRL 26	Pons	M	40 + 1	1617.83	8.39
CTRL 27	Obex	F	23 + 4	1978.02	6.96
CTRL 28	Pons	F	32 + 0	1721.97	4.42
CTRL 29	Brainstem *in toto*	F	22 + 0	1910.65	4.68
CTRL 30	Brainstem *in toto*	M	18 + 0	2319.90	9.57
CTRL 31	Obex	F	29 + 0	3565.39	7.83
CTRL 32	Obex, Pons	F	41 + 4	1530.56	7.49

variants in 6 individuals) compared with those with CCS anomalies (106 variants in 28 individuals; $p = 0.024$). In contrast, no statistically significant differences in mutational burden were observed when samples were stratified by sex ($p = 0.12$) or by severity of brainstem lesions ($p = 0.58$). Specifically, 119 variants were identified in 21 males and 39 in 13 females, while 129 variants were detected in 29 individuals with severe lesions and 29 variants in 5 individuals with mild lesions.

Using a combination of ACMG classification criteria, population frequency data, *in silico* prediction scores, sequencing metrics, and literature evidence, we selected three mtDNA variants of interest (Table 3): 1) m.3323 T > C (p.Leu6Pro), a heteroplasmic missense variant in *MT-ND1* (sample SB25; variant allele frequency [VAF]: 0.025), classified as variant of uncertain significance (VUS); 2) m.3243A > T (rs199474657), a heteroplasmic non-coding variant in *MT-TL1* (sample SB26; VAF:0.014), classified as likely pathogenic and previously associated with varying neurological phenotypes (Alston et al., 2010); 3) m.3308 T > C (p.Met1Thr) (rs28358582), a homoplasmic start-loss variant in *MT-ND1* (sample SB29; VAF: 0.995), classified as benign according to current ACMG guidelines but previously reported in association with sudden infant death syndrome (SIDS) and left ventricular hypertrabeculation/noncompaction (LVNC) (Opdal et al., 1999; Zarrouk Mahjoub et al., 2011). The homoplasmic m.3308 T > C variant was detected in the corresponding unaffected tissue, consistent with a germline origin, while the other two variants, present at very low heteroplasmic levels, were considered likely somatic. No pathogenic mtDNA copy number variants (CNVs) were identified.

Haplogroup analysis with Haplogrep 3 revealed two predominant mitochondrial haplogroups in the SB cohort: haplogroup H in 17 individuals (17/34, 50%) and haplogroup U in 5 individuals (5/34, 15%). Additional haplogroups observed included: K (3/34, 9%), J (2/34, 6%), L (2/34, 6%), T (2/34, 6%), M (1/34, 3%), V (1/34, 3%), and W (1/34, 3%) (Table 1). These findings are consistent with the haplogroup distribution observed in the TSI dataset, where haplogroup H was detected in 52/107 (49%) individuals, and haplogroup U in 15/107 (14%). Additional haplogroups included T (14/107, 13%), K (9/107, 8%), J (8/107, 7%), W (4/107, 4%), V (2/107, 2%), D (1/107, 1%), L (1/107, 1%), and X (1/107, 1%).

3.2. mtDNA copy number (mtDNA-CN)

Quantification of mtDNA-CN by qPCR revealed significantly higher levels in affected brainstem tissues (mean: 9695.54 copies) compared with both control brainstem tissues (mean: 1786.70 copies; $p < 0.0001$) and unaffected tissues (mean: 2994.35 copies; $p = 0.005$) (Fig. 1, Table 1, and Table 2).

Notably, brainstem tissues with mild anomalies exhibited higher mtDNA-CN levels than those with severe anomalies (mean: 14,734 vs. 8,658; $p = 0.02$) (Fig. 1 and Table 1). Both groups with mild and severe anomalies showed significantly higher mtDNA-CN compared with control brainstem tissues ($p < 0.0001$). In contrast, mtDNA-CN did not differ significantly between affected brainstem tissues from males and females ($p = 0.25$) or between tissues from SB cases with and without CCS defects ($p = 0.61$). Additionally, no statistically significant difference was observed between control brainstem tissues and unaffected tissues ($p = 0.62$) (Fig. 1).

3.3. mtDNA methylation and D-loop instability

MS-HRM analysis showed significantly higher D-loop methylation levels in affected brainstem tissues (mean: 9.49%) compared with both control brainstem tissues (mean: 7.37%; $p < 0.0001$) and unaffected tissues (mean: 7.56%; $p = 0.0001$) (Fig. 2, Table 1, and Table 2). On the contrary, no significant differences in methylation levels were observed between controls and unaffected tissues ($p = 0.68$), and when stratifying by sex ($p = 0.0995$), presence or absence of CCS anomalies ($p = 0.7440$), or severity of brainstem lesions ($p = 0.8948$).

Analysis of the hypervariable D310 region (C7-T-C5; chrM:303–315) revealed alterations of the poly(C) tract sequence in 15 of 41 affected brainstem tissues (37%) compared with unaffected tissues in SB cases, suggestive of D-loop instability (Table S1). The most frequently observed altered sequence motif was C8-C-C6, detected in 6 samples (40%), followed by C8-T-C6 and C8-T-C5, each observed in two samples (13%). Less frequent combinations included C9-C-C6, C7-GA-C6, C7-CC-C6, C8-TT-C6, and C7-T-C6, each found in a single case.

Table 3
Relevant mitochondrial variants identified in affected brainstem tissues.

Gene	Variant type	Zigosity	Variant	VAF	Read depth	gnomAD v4.1.0 frequency (%)	MITOMAP frequency (%)	ACMG (criteria)	ClinVar	APOGEE score	HmtVar score
MT-ND1	Missense	Heteroplasmic	m.3323T>C ENST00000361390.2: c.17T>C p.(Leu6Pro)	0.0248447	644 (16/628)	0.001772	0	VUS (0 p) (PM2_p, BP4_p)		0.205	0.8
MT-TL1	Non-coding	Heteroplasmic	m.3243A>T	0.0135501	738 (10/728)	0 (rs199474657)	0	LP (7 p) (PS3_m, PS4_m, PM2_p, PM5_p, PP3_p)	LP		
MT-ND1	Start-loss	Homoplasmic	m.3308T>C ENST00000361390.2: c.2T>C p.(Met1Thr)	0.995169	1449 (1442/7)	2.852 (rs28358582)	0.721	B (-9 p) (BA1_vs, BP4_p)	B/LB	0.328	

_p: supporting; _m: moderate; _vs: very strong; p: points; LP: likely pathogenic; VUS: variant of uncertain significance; B: benign; LB: likely benign.

4. Discussion

In this study, we analyzed mtDNA alterations in a cohort of 42 SB cases with brainstem and CCS anomalies. Our findings provide further evidence supporting the role of mitochondrial dysfunction in the pathogenesis of SB.

We observed a significant increase in mtDNA-CN in affected brainstem tissues compared with both control brainstem tissues and unaffected tissues. Increased mtDNA mutational load has been reported in the brains of individuals with schizophrenia (Bulduk et al., 2024) and Alzheimer's disease (Lin et al., 2002) compared with healthy controls. Furthermore, D'Erchia et al. (2015) reported mtDNA-CN values in normal adult brain tissues ranging from 772.48 to 2520.35, with a mean value of 1897.24. This range closely overlaps with mean mtDNA-CN observed in our controls (1786.70) and, partially, in unaffected tissues (2994.35), whereas it is substantially lower than the levels observed in affected brainstem samples (9695.54). Interestingly, the increase of mtDNA-CN observed in SBs with mild brainstem lesions, compared with those with severe lesions, recapitulates the trend observed by Danusso and colleagues (2022) in SIDS. This pattern may reflect a compensatory response to cellular injury or metabolic/oxidative stress, where cells upregulate mitochondrial biogenesis, thereby increasing mtDNA-CN, to counteract the mitochondrial dysfunction. Similar compensatory increases have been documented in SIUDS (Lattuada et al., 2018) and placental tissues from women with gestational diabetes mellitus (Qiu et al., 2013). Conversely, under conditions of more severe cellular injury, mitochondrial damage may exceed the capacity of compensatory mechanisms, leading to impaired mtDNA replication/maintenance and a consequent reduction in mtDNA-CN, as reported, for example, in experimental models of ischemia–reperfusion injury (Zhang et al., 2022a).

In unaffected tissues, and to some extent in affected brainstem tissues, we observed a few outlier samples exhibiting particularly high mtDNA-CN. Previous studies in both humans and mice have shown that mtDNA-CN can vary dramatically not only across different bodily districts but also within the same tissue, with the heart exhibiting the highest variability among tissues (Rath et al., 2024). This variability may partly account for the differences observed in our cohort, as two outliers among unaffected tissues correspond to heart samples (SB32 and SB37), and mtDNA-CN analysis was performed on different portions of the brainstem depending on tissue availability.

The instability of the hypervariable D310 region, observed in 37% of brainstem lesions, may indicate a dynamic and potentially dysfunctional mitochondrial environment in the affected fetuses. The critical role of the D-loop in brain mitochondrial metabolism is supported by multiple studies linking D-loop instability to various brain tumors (Altafi et al., 2019), including meningioma (Mohamed Yusoff et al., 2020) and glioblastoma (Szmyd et al., 2024). Furthermore, the significantly increased levels of D-loop methylation in brainstem lesions compared with both brainstem controls and unaffected tissues suggest a role for mitochondrial epigenetic regulation in fetal demise. Previous studies on individuals with other neurological disorders, such as Alzheimer's disease (Stoccoro et al., 2022) and Aicardi-Goutières syndrome (AGS), a severe early-onset encephalopathy (Dragoni et al., 2023), have also reported increased D-loop methylation compared with healthy controls. Since the D-loop region contains the origin of mtDNA replication and transcription, its methylation levels are predominantly inversely correlated with mtDNA-CN (Zhang et al., 2022b; Yin and Guo, 2025; Chung et al., 2019). Interestingly, our study revealed concurrent increases in D-loop methylation and mtDNA-CN in the SB brainstem tissues. A similar trend was reported by Dragoni et al. (2023) in children affected by AGS. Further investigations are required to clarify the mechanisms underlying the positive correlation between mtDNA methylation and mtDNA-CN. This may reflect the involvement of specific methylation-related enzymes (e.g., DNMT1, DNMT3A/B, and TET), which translocate from the nucleus to mitochondria and modulate mtDNA methylation (Yin and

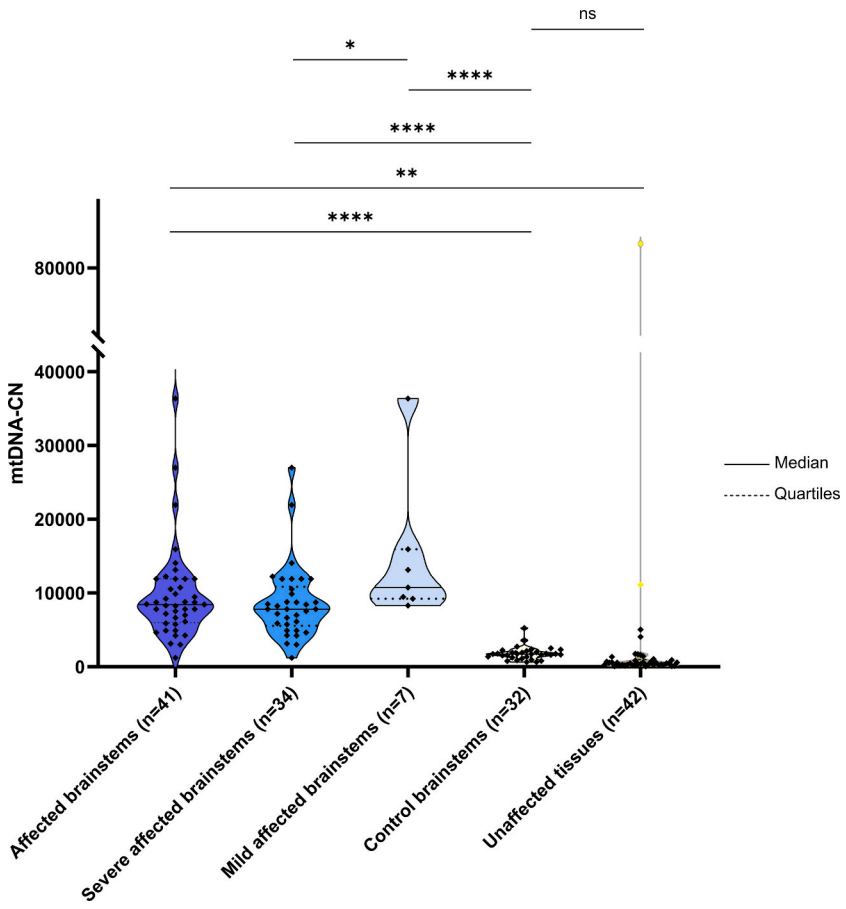

Fig. 1. Analysis of absolute mitochondrial DNA copy number (mtDNA-CN). mtDNA-CN detected in affected brainstem tissues (overall), severely and mildly affected brainstems (stratified), control brainstem tissues, and unaffected tissues. The two outliers, represented as yellow diamonds in the unaffected tissues, correspond to two cardiac tissue samples. * $p = 0.02$, ** $p = 0.005$, **** $p < 0.0001$, ns = not significant. (For interpretation of the references to colour in this figure legend, the reader is referred to the web version of this article.)

Guo, 2025; Dou et al., 2019; Shock et al., 2011). In a recent study, Chi et al. (2025) reported a concomitant increase in mtDNA-CN and D-loop methylation levels, along with a positive correlation between *POLG* promoter methylation and mtDNA-CN. Additionally, altered expression of nuclear factors critical for mtDNA maintenance, including DNA polymerase γ, TWINKLE, and TFAM, may also contribute to mtDNA alterations (Milenkovic et al., 2013; Ekstrand et al., 2004; Kelly et al., 2012). These findings highlight a potentially relevant crosstalk between nuclear and mitochondrial epigenetic networks involved in mitochondrial biogenesis.

Analysis of mtDNA mutational burden revealed a significant enrichment of mtDNA variants in SB cases lacking CCS anomalies compared with those presenting CCS defects. The enrichment of mtDNA variants in the first subgroup supports mitochondrial dysfunction as a relevant pathogenic mechanism contributing to fetal demise, even in the absence of other overt abnormalities.

In this study, unaffected tissues, primarily thymus, from SBs with brainstem abnormalities were also examined for intra-individual comparison. Although different tissue types may have varying energy requirements, mtDNA-CN and D-loop methylation levels were statistically comparable between "extra-brainstem" unaffected tissues and brainstem control tissues, suggesting a regional specificity of mitochondrial alterations in abnormal brainstem tissues of SBs and a potential multifactorial interplay between localized neuropathological damage and mitochondrial genomic and epigenetic imbalances contributing to fetal death.

In conclusion, our findings and previous studies support the role of mitochondrial dysfunction as a biological hallmark in SB. Moreover, these data underscore the potential utility of mitochondrial DNA content and D-loop (hyper)methylation as early biomarkers of fetal demise. Importantly, they also offer new insights into the fundamental biology of mitochondrial DNA in the brainstem, a tissue that is not represented in widely used public datasets such as GTEx (Genotype-Tissue Expression).

Ethical statement

All cases included in the present study followed the ethical measures guaranteed by the Ministry of Health in accordance with Italian Law n.31/2006 "Regulations for Diagnostic Postmortem Investigation in Victims of SIDS and Unexpected Fetal Death", which decrees that all fetuses who died without any apparent cause must be submitted to a thorough diagnostic post-mortem investigation.

Funding

This research was partly funded by a research grant from "SUID & SIDS Italia Onlus" awarded to EE.

CRediT authorship contribution statement

Mauro Lecca: Writing – review & editing, Writing – original draft, Visualization, Validation, Software, Investigation, Formal analysis, Data curation. **Nicolò Mele:** Writing – review & editing, Writing – original draft, Investigation, Formal analysis, Data curation. **Patrizia Leonardi:** Writing – original draft, Investigation, Formal analysis. **Giulia Ottaviani:** Writing – review & editing, Writing – original draft, Supervision,

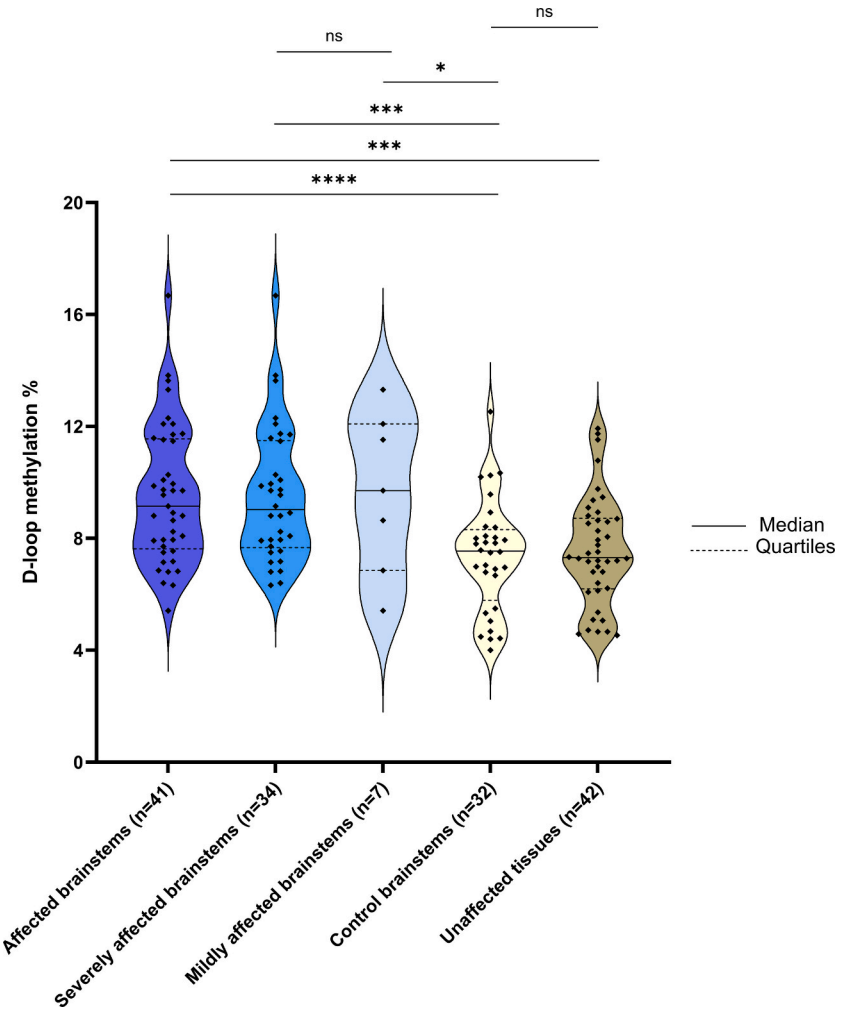

Fig. 2. Analysis of D-loop methylation. D-loop methylation percentages detected in affected brainstem tissues (overall), severely and mildly affected brainstems (stratified), control brainstem tissues, and unaffected tissues. Methylation analysis was performed by MS-HRM (Methylation-Sensitive High-Resolution Melting). * $p = 0.016$; *** $p = 0.0001$; **** $p < 0.0001$, ns = not significant.

Investigation, Funding acquisition, Data curation. **Edoardo Errichiello:** Writing – review & editing, Writing – original draft, Visualization, Validation, Supervision, Resources, Project administration, Methodology, Investigation, Funding acquisition, Formal analysis, Data curation, Conceptualization.

Declaration of Competing Interest

The authors declare that they have no known competing financial interests or personal relationships that could have appeared to influence the work reported in this paper.

Acknowledgments

We would like to thank all families involved in this study. This research project was partly funded by a grant from “SUID & SIDS Italia Onlus” awarded to EE.

Appendix A. Supplementary data

Supplementary data to this article can be found online at https://doi.org/10.1016/j.mito.2026.102152.

References

Stanley, K.E., Giordano, J., Thorsten, V., Buchovecky, C., Thomas, A., Ganapathi, M., Liao, J., Dharmadhikari, A.V., Revah-Politi, A., Ernst, M., Lippa, N., Holmes, H., Povysil, G., Hostyk, J., Parker, C.B., Goldenberg, R., Saade, G.R., Dudley, D.J., Pinar, H., Hogue, C., Goldstein, D.B., 2020. Causal Genetic Variants in Stillbirth. N. Engl. J. Med. 383 (12), 1107–1116. https://doi.org/10.1056/NEJMoa1908753.

Dolanc Merc, M., Peterlin, B., Lovrecic, L., 2023. The genetic approach to stillbirth: a “systematic review”. Prenat. Diagn. 43 (9), 1220–1228. https://doi.org/10.1002/pd.6354.

Giorlandino, C., Mesoraca, A., Cignini, P., 2012. Sudden intrauterine unexplained death: time for change. J Prenat Med. 6 (4), 57–59.

Lavezzi, A.M., Ferrero, S., Matturri, L., Roncati, L., Pusiol, T., 2016. Developmental neuropathology of brainstem respiratory centers in unexplained stillbirth: What's the meaning? International Journal of Developmental Neuroscience: the Official Journal of the International Society for Developmental Neuroscience 53, 99–106. https://doi.org/10.1016/j.ijdevneu.2016.06.007.

Ottaviani, G., 2016. Defining Sudden Infant Death and Sudden Intrauterine Unexpected Death Syndromes with Regard to Anatomo-Pathological Examination. Front. Pediatr. 4, 103. https://doi.org/10.3389/fped.2016.00103.

Lattuada, D., Alfonsi, G., Roncati, L., Pusiol, T., Bulfoni, A., Ferrero, S., Lavezzi, A.M., 2018. Mitochondrial DNA content: a new biomarker for sudden intrauterine unexplained death syndrome (SIUDS). Mitochondrion 40, 13–15. https://doi.org/10.1016/j.mito.2017.09.001.

Karaa, A., Elsharkawi, I., Clapp, M.A., Balcells, C., 2019. Effects of mitochondrial disease/dysfunction on pregnancy: a retrospective study. Mitochondrion 46, 214–220. https://doi.org/10.1016/j.mito.2018.06.007.

Feeney, C.L., Lim, A.Z., Fagan, E., Blain, A., Bright, A., Maddison, J., Devine, H., Stewart, J., Taylor, R.W., Gorman, G.S., Turnbull, D.M., Nesbitt, V., McFarland, R., 2019. A case-comparison study of pregnant women with mitochondrial disease - what to expect? BJOG: an International Journal of Obstetrics and Gynaecology 126 (11), 1380–1389. https://doi.org/10.1111/1471-0528.15667.

Hui, L., Hayman, P., Buckland, A., Fahey, M.C., Mackey, D.A., Mallett, A.J., Schweitzer, D.R., Stuart, C.P., Yau, W.Y., Christodoulou, J., 2025. Pregnancy in women with mitochondrial disease-a literature review and suggested guidance for preconception and pregnancy care. Aust. N. Z. J. Obstet. Gynaecol. 65 (1), 30–36. https://doi.org/10.1111/ajo.13874.

Vanniarajan, A., Govindaraj, P., Carlus, S.J., Aruna, M., Aruna, P., Kumar, A., Jayakar, R. I., Lionel, A.C., Gupta, S., Rao, L., Gupta, N.J., Chakravarthy, B., Deenadayal, M., Selvaraj, K., Andal, S., Reddy, B.M., Singh, L., Thangaraj, K., 2011. Mitochondrial DNA variations associated with recurrent pregnancy loss among Indian women. Mitochondrion 11 (3), 450–456. https://doi.org/10.1016/j.mito.2011.01.002.

Seyedhassani, S.M., Houshmand, M., Kalantar, S.M., Modabber, G., Aflatoonian, A., 2010. No mitochondrial DNA deletions but more D-loop point mutations in repeated pregnancy loss. J. Assist. Reprod. Genet. 27 (11), 641–648. https://doi.org/10.1007/s10815-010-9435-2.

Danusso, R., Alfonsi, G., Ferrero, S., Lavezzi, A.M., Lattuada, D., 2022. Mitochondrial DNA content: a new potential biomarker for Sudden Infant Death Syndrome. Pediatr. Res. 92 (5), 1282–1287. https://doi.org/10.1038/s41390-021-01901-z.

Diez-Juan, A., Rubio, C., Marin, C., Martinez, S., Al-Asmar, N., Riboldi, M., Díaz-Gimeno, P., Valbuena, D., Simón, C., 2015. Mitochondrial DNA content as a viability score in human euploid embryos: less is better. Fertil. Steril. 104 (3), 534. https://doi.org/10.1016/j.fertnstert.2015.05.022.

Ye, M., Shi, W., Hao, Y., Zhang, L., Chen, S., Wang, L., He, X., Li, S., Xu, C., 2020. Associations of mitochondrial DNA copy number and deletion rate with early pregnancy loss. Mitochondrion 55, 48–53. https://doi.org/10.1016/j.mito.2020.07.006.

Lavezzi, A.M., Ottaviani, G., Mauri, M., Matturri, L., 2004. Hypoplasia of the arcuate nucleus and maternal smoking during pregnancy in sudden unexplained perinatal and infant death. Neuropathology : Official Journal of the Japanese Society of Neuropathology 24 (4), 284–289. https://doi.org/10.1111/j.1440-1789.2004.00558.x.

Matturri, L., Mauri, M., Ferrero, M.E., Lavezzi, A.M., 2008. Unexpected perinatal loss versus Sids-a common neuropathologic entity. The Open Neurology Journal 2, 45–50. https://doi.org/10.2174/1874205X00802010045.

Paradiso, B., Ferrero, S., Thiene, G., Lavezzi, A.M., 2018. Variability of the medullary arcuate nucleus in humans. Brain and Behavior 8 (11), e01133. https://doi.org/10.1002/brb3.1133.

Preste, R., Vitale, O., Clima, R., Gasparre, G., Attimonelli, M., 2019. HmtVar: a new resource for human mitochondrial variations and pathogenicity data. Nucleic Acids Res. 47 (D1), D1202–D1210. https://doi.org/10.1093/nar/gky1024.

Bianco, S.D., Parca, L., Petrizzelli, F., Biagini, T., Giovannetti, A., Liorni, N., Napoli, A., Carella, M., Procaccio, V., Lott, M.T., Zhang, S., Vescovi, A.L., Wallace, D.C., Caputo, V., Mazza, T., 2023. APOGEE 2: multi-layer machine-learning model for the interpretable prediction of mitochondrial missense variants. Nat. Commun. 14 (1), 5058. https://doi.org/10.1038/s41467-023-40797-7.

Sonney, S., Leipzig, J., Lott, M.T., Zhang, S., Procaccio, V., Wallace, D.C., Sondheimer, N., 2017. Predicting the pathogenicity of novel variants in mitochondrial tRNA with MitoTIP. PLoS Comput. Biol. 13 (12), e1005867. https://doi.org/10.1371/journal.pcbi.1005867.

McCormick, E.M., Lott, M.T., Dulik, M.C., Shen, L., Attimonelli, M., Vitale, O., Karaa, A., Bai, R., Pineda-Alvarez, D.E., Singh, L.N., Stanley, C.M., Wong, S., Bhardwaj, A., Merkurjev, D., Mao, R., Sondheimer, N., Zhang, S., Procaccio, V., Wallace, D.C., Gai, X., Falk, M.J., 2020. Specifications of the ACMG/AMP standards and guidelines for mitochondrial DNA variant interpretation. Hum. Mutat. 41 (12), 2028–2057. https://doi.org/10.1002/humu.24107.

Schönherr, S., Weissensteiner, H., Kronenberg, F., Forer, L., 2023. Haplogrep 3 - an interactive haplogroup classification and analysis platform. Nucleic Acids Res. 51 (W1), W263–W268. https://doi.org/10.1093/nar/gkad284.

Xu, C., Tran-Thanh, D., Ma, C., May, K., Jung, J., Vecchiarelli, J., Done, S.J., 2012. Mitochondrial D310 mutations in the early development of breast cancer. Br. J. Cancer 106 (9), 1506–1511. https://doi.org/10.1038/bjc.2012.74.

Errichiello, E., Balsamo, A., Cerni, M., Venesio, T., 2015. Mitochondrial variants in MT-CO2 and D-loop instability are involved in MUTYH-associated polyposis. J. Mol. Med. (Berl) 93 (11), 1271–1281. https://doi.org/10.1007/s00109-015-1312-0.

Stoccoro, A., Baldacci, F., Ceravolo, R., Giampietri, L., Tognoni, G., Siciliano, G., Migliore, L., Coppedè, F., 2022. Increase in Mitochondrial D-Loop Region Methylation Levels in Mild Cognitive Impairment individuals. Int. J. Mol. Sci. 23 (10), 5393. https://doi.org/10.3390/ijms23105393.

Migheli, F., Stoccoro, A., Coppedè, F., Wan Omar, W.A., Failli, A., Consolini, R., Seccia, M., Spisni, R., Miccoli, P., Mathers, J.C., Migliore, L., 2013. Comparison study of MS-HRM and pyrosequencing techniques for quantification of APC and CDKN2A gene methylation. PLoS One 8 (1), e52501. https://doi.org/10.1371/journal.pone.0052501.

Alston, C.L., Bender, A., Hargreaves, I.P., Mundy, H., Deshpande, C., Klopstock, T., McFarland, R., Horvath, R., Taylor, R.W., 2010. The pathogenic m.3243A>T mitochondrial DNA mutation is associated with a variable neurological phenotype. Neuromuscular Disorders: NMD 20 (6), 403–406. https://doi.org/10.1016/j.nmd.2010.04.003.

Opdal, S.H., Rognum, T.O., Torgersen, H., Vege, A., 1999. Mitochondrial DNA point mutations detected in four cases of sudden infant death syndrome. Acta paediatrica (Oslo, Norway : 1992), 88(9), 957–960. https://doi.org/10.1080/08035259950168441.

Zarrouk Mahjoub, S., Mehri, S., Ourda, F., Boussaada, R., Mechmeche, R., Arab, S.B., Finsterer, J., 2011. Transition m.3308T>C in the ND1 gene is associated with left ventricular hypertrabeculation/noncompaction. Cardiology 118 (3), 153–158. https://doi.org/10.1159/000328002.

Bulduk, B.K., Tortajada, J., Valiente-Pallejà, A., Callado, L.F., Torrell, H., Vilella, E., Meana, J.J., Muntané, G., Martorell, L., 2024. High number of mitochondrial DNA alterations in postmortem brain tissue of patients with schizophrenia compared to healthy controls. Psychiatry Res. 337, 115928. https://doi.org/10.1016/j.psychres.2024.115928.

Lin, M.T., Simon, D.K., Ahn, C.H., Kim, L.M., Beal, M.F., 2002. High aggregate burden of somatic mtDNA point mutations in aging and Alzheimer's disease brain. Hum. Mol. Genet. 11 (2), 133–145. https://doi.org/10.1093/hmg/11.2.133.

D'Erchia, A.M., Atlante, A., Gadaleta, G., Pavesi, G., Chiara, M., De Virgilio, C., Manzari, C., Mastropasqua, F., Prazzoli, G.M., Picardi, E., Gissi, C., Horner, D., Reyes, A., Sbisà, E., Tullo, A., Pesole, G., 2015. Tissue-specific mtDNA abundance from exome data and its correlation with mitochondrial transcription, mass and respiratory activity. Mitochondrion 20, 13–21. https://doi.org/10.1016/j.mito.2014.10.005.

Qiu, C., Hevner, K., Abetew, D., Sedensky, M., Morgan, P., Enquobahrie, D.A., Williams, M.A., 2013. Mitochondrial DNA copy number and oxidative DNA damage in placental tissues from gestational diabetes and control pregnancies: a pilot study. Clin. Lab. 59 (5–6), 655–660. https://doi.org/10.7754/clin.lab.2012.120227.

Zhang, Z., Yang, D., Zhou, B., Luan, Y., Yao, Q., Liu, Y., Yang, S., Jia, J., Xu, Y., Bie, X., Wang, Y., Li, Z., Li, A., Zheng, H., He, Y., 2022a. Decrease of MtDNA copy number affects mitochondrial function and involves in the pathological consequences of ischaemic stroke. J. Cell Mol. Med. 26 (15), 4157–4168. https://doi.org/10.1111/jcmm.17262.

Rath, S.P., Gupta, R., Todres, E., Wang, H., Jourdain, A.A., Ardlie, K.G., Calvo, S.E., Mootha, V.K., 2024. Mitochondrial genome copy number variation across tissues in mice and humans. Proceedings of the National Academy of Sciences of the United States of America 121 (33), e2402291121. https://doi.org/10.1073/pnas.2402291121.

Altafi, D., Sadeghi, S., Hojatian, H., Torabi Afra, M., Pakizeh Kar, S., Gorji, M., Houshmand, M., 2019. Mitochondrial Polymorphisms, in the D-Loop Area, are Associated with Brain Tumors. Cell J. 21 (3), 350–356. https://doi.org/10.22074/cellj.2019.5947.

Mohamed Yusoff, A.A., Mohd Khair, S.Z.N., Wan Abdullah, W.S., Abd Radzak, S.M., Abdullah, J.M., 2020. Somatic mitochondrial DNA D-loop mutations in meningioma discovered: a preliminary data. J. Cancer Res. Ther. 16 (6), 1517–1521. https://doi.org/10.4103/jcrt.JCRT_1132_16.

Szmyd, B., Stanisławska, P., Podstawka, M., Zaczkowski, K., Izbiński, P.M., Kulczycka-Wojdala, D., Stawski, R., Wiśniewski, K., Janczar, K., Braun, M., Białasiewicz, P., Jaskólski, D.J., Bobeff, E.J., 2024. D-Loop Mutations as Prognostic Markers in Glioblastoma-a pilot Study. Int. J. Mol. Sci. 25 (8), 4334. https://doi.org/10.3390/ijms25084334.

Dragoni, F., Garau, J., Orcesi, S., Varesio, C., Bordoni, M., Scarian, E., Di Gerlando, R., Fazzi, E., Battini, R., Gjurgjaj, A., Rizzo, B., Pansarasa, O., Gagliardi, S., 2023. Comparison between D-loop methylation and mtDNA copy number in patients with Aicardi-Goutières Syndrome. Front. Endocrinol. 14, 1152237. https://doi.org/10.3389/fendo.2023.1152237.

Zhang, J., Shang, J., Wang, F., Huo, X., Sun, R., Ren, Z., Wang, W., Yang, M., Li, G., Gao, D., Liu, R., Bai, P., Wang, S., Wang, Y., Yan, X., 2022b. Decreased mitochondrial D-loop region methylation mediates an increase in mitochondrial DNA copy number in CADASIL. Clin. Epigenetics 14 (1), 2. https://doi.org/10.1186/s13148-021-01225-z.

Yin, M.T., Guo, L., 2025. Mitochondrial DNA methylation: State-of-the-art in molecular mechanisms and disease implications. Journal of advanced research, S2090-1232 (25)00644-7. Advance online publication. https://doi.org/10.1016/j.jare.2025.08.029.

Chung, J.K., Lee, S.Y., Park, M., Joo, E.J., Kim, S.A., 2019. Investigation of mitochondrial DNA copy number in patients with major depressive disorder. Psychiatry Res. 282, 112616. https://doi.org/10.1016/j.psychres.2019.112616.

Dou, X., Boyd-Kirkup, J.D., McDermott, J., Zhang, X., Li, F., Rong, B., Zhang, R., Miao, B., Chen, P., Cheng, H., Xue, J., Bennett, D., Wong, J., Lan, F., Han, J.J., 2019. The strand-biased mitochondrial DNA methylome and its regulation by DNMT3A. Genome Res. 29 (10), 1622–1634. https://doi.org/10.1101/gr.234021.117.

Shock, L.S., Thakkar, P.V., Peterson, E.J., Moran, R.G., Taylor, S.M., 2011. DNA methyltransferase 1, cytosine methylation, and cytosine hydroxymethylation in mammalian mitochondria. PNAS 108 (9), 3630–3635. https://doi.org/10.1073/pnas.1012311108.

Chi, H., Shu, H., Yang, Y., Ikeno, Y., Wu, J., Wang, Z., Zare, H., Alexeyev, M., Bai, Y., 2025. Elevated mtDNA copy number in older adults is linked to methylation of mitochondrial and nuclear regulatory regions. GeroScience. https://doi.org/10.1007/s11357-025-02037-2.

Milenkovic, D., Matic, S., Kühl, I., Ruzzenente, B., Freyer, C., Jemt, E., Park, C.B., Falkenberg, M., Larsson, N.G., 2013. TWINKLE is an essential mitochondrial helicase required for synthesis of nascent D-loop strands and complete mtDNA replication. Hum. Mol. Genet. 22 (10), 1983–1993. https://doi.org/10.1093/hmg/ddt051.

Ekstrand, M.I., Falkenberg, M., Rantanen, A., Park, C.B., Gaspari, M., Hultenby, K., Rustin, P., Gustafsson, C.M., Larsson, N.G., 2004. Mitochondrial transcription factor a regulates mtDNA copy number in mammals. Hum. Mol. Genet. 13 (9), 935–944. https://doi.org/10.1093/hmg/ddh109.

Kelly, R.D., Mahmud, A., McKenzie, M., Trounce, I.A., St John, J.C., 2012. Mitochondrial DNA copy number is regulated in a tissue specific manner by DNA methylation of the nuclear-encoded DNA polymerase gamma a. Nucleic Acids Res. 40 (20), 10124–10138. https://doi.org/10.1093/nar/gks770.